Science of the Total Environment 783 (2021) 146915

Contents lists available at ScienceDirect

Science of the Total Environment

journal homepage: www.elsevier.com/locate/scitotenv

In vitro toxic synergistic effects of exogenous pollutants-trimethylamine and its metabolites on human respiratory tract cells

Zhilin Qiu [a], Guiying Li [a,b,*], Taicheng An [a,b]

[a] Guangdong-Hong Kong-Macao Joint Laboratory for Contaminants Exposure and Health, Guangdong Key Laboratory of Environmental Catalysis and Health Risk Control, Institute of Environmental Health and Pollution control, Guangdong University of Technology, Guangzhou 510006, China
[b] Guangzhou Key Laboratory of Environmental Catalysis and Pollution Control, Key Laboratory of City Cluster Environmental Safety and Green Development (Department of Education, China), School of Environmental Science and Engineering, Guangdong University of Technology, Guangzhou 510006, China

HIGHLIGHTS

- Trimethylamine (TMA) induced cell viability decrease & ROS increase in 16HBE cell.
- Dimethylamine was found to be the main product of TMA metabolized by 16HBE cells.
- TMA metabolism included N-formylation and hydroxylation mediated by CYP enzymes.
- Metabolites of TMA were more toxic and contributed to cytotoxicity together with TMA.

GRAPHICAL ABSTRACT

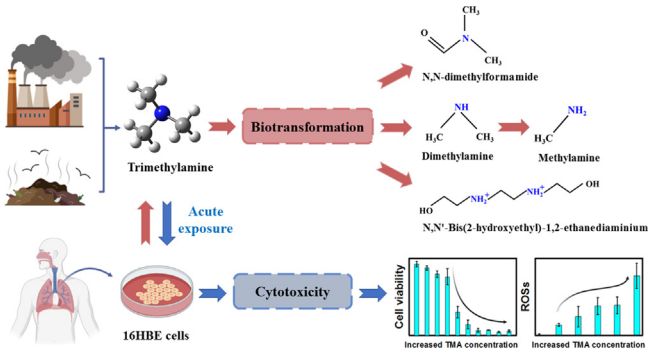

ARTICLE INFO

Article history:
Received 21 February 2021
Received in revised form 29 March 2021
Accepted 30 March 2021
Available online 6 April 2021

Editor: Daqiang Yin

Keywords:
Trimethylamine
Respiratory tract cells
Metabolic mechanism
ROS generation
Cytochrome P450 enzymes

ABSTRACT

The wide presence of volatile organic amines in atmosphere has been clarified to relate to adverse effects on human respiratory health. However, toxic effects of them on human respiratory tract and their metabiotic mechanism of in vivo transformation have not been elucidated yet. Herein, cell viability and production of reactive oxygen species (ROSs) were first investigated during acute exposure of trimethylamine (TMA) to bronchial epithelial cells (16HBE), along with identification of toxic metabolites and metabolic mechanisms of TMA from headspace atmosphere and cell culture. Results showed that cell activity decreased and ROS production increased with raising exposure TMA concentration. Toxic effects may be induced not only by TMA itself, but also more likely by its cellular metabolites. Increased dimethylamine identified in headspace atmosphere and cell solution was the main metabolite of TMA, and methylamine was also confirmed to be a further metabolite. In addition, TMA can also be oxygenated to generate *N*,*N*-dimethylformamide and *N*,*N*′-Bis(2-hydroxyethyl)-1,2-ethanediaminium by N-formylation or hydroxylation, which was considered to be the participation of cytochrome P450 (CYP) enzymes. Overall, we can conclude that respiratory tract cells may produce more toxic metabolites during exposure of toxic organic amines, which together further induce cellular oxidative stress and necrosis. Hence, the environment and health impact of metabolites as well as original parent atmospheric organic amines should be paid more attention in further researches and disease risk assessments.

* Corresponding author at: Guangdong-Hong Kong-Macao Joint Laboratory for Contaminants Exposure and Health, Guangdong Key Laboratory of Environmental Catalysis and Health Risk Control, Institute of Environmental Health and Pollution control, Guangdong University of Technology, Guangzhou 510006, China.
E-mail address: ligy1999@gdut.edu.cn (G. Li).

https://doi.org/10.1016/j.scitotenv.2021.146915
0048-9697/

1. Introduction

Trimethylamine (TMA), a typical tertiary amine, is not only the most commonly emitted amine from various sources, but also the most abundant amine in the atmosphere, with a flux of 169 ± 33 Gg N a^{-1} (Ge et al., 2011; Kamarulzaman et al., 2019). As reported, the average concentration of TMA from an industrial fishery complex was approximately 20.60 ppb with a maximum concentration of 72.30 ppb (Seo et al., 2011), which was greatly higher than the odor threshold of TMA (from 0.21 to 0.58 ppb) (USEPA, 2009). Moreover, due to high photochemical conversion activity, TMA can react with atmospheric nitrogen oxides to produce carcinogens such as formaldehyde, dimethylnitrosamine and dimethylnitramine under irradiation of natural sunlight (Pitts et al., 1978). In the presence of nitrate radicals in the air (Silva et al., 2008), or sulfuric acid at the air-particle interface (Zhang et al., 2019; Zhang et al., 2021; Zhao et al., 2020), several amines also promote the formation of secondary aerosol particles, which then determines their atmospheric lifetime.

The respiratory tract, a major entrance of exogenous pollutants into the body, is exposed continuously to the airborne environmental chemicals in gaseous or aerosol state (Dahl et al., 1988; Foth, 1995). Inhalation is the overriding exposure route of volatile TMA, a xenobiotic for the human body, representing that respiratory tract is the dominant target for chemically induced toxicity of TMA. Recent researches showed that TMA at concentrations higher than 20 ppm could induce upper respiratory tract irritation in humans, and exposing to TMA of 750 ppm could cause alveolar emphysema, tracheal inflammation and necrosis in rats (American, 2005; Kinney et al., 1990). Therefore, the respiratory epithelium is susceptible to hazardous effects of inhaled compounds.

On the other hand, the respiratory tract has the capacity to metabolize xenobiotics, which is closely related to the toxic effects of xenobiotics entering the body and the pathogenesis of lung diseases such as lung cancer and chronic obstructive pulmonary disease. Metabolic processes of xenobiotics in the respiratory tract require the catalytic activation of related enzymes, and cytochrome P450 (CYP) enzymes in extrahepatic tissues often play a dominant role in metabolic activation of xenobiotics (Serabjit-Singh et al., 1980; Stading et al., 2020). Several CYPs, including CYP2F1, CYP4B1 and CYP2A6, may be involved in the metabolic activation of 3-methylindole in human lung microsomes (Ruangyuttikarn et al., 1991). CYP1A1 appears to be the efficient enzyme in the metabolic activation of aromatic hydrocarbons in human lung, such as 5-methylchrysene and 6-methylchrysene (Koehl et al., 1996). Besides CYP enzymes, other oxidoreductases can also metabolize xenobiotics. Flavin-containing monooxygenases in lungs can oxidize and metabolize a variety of xenobiotics containing nitrogen, sulfur and phosphorus, some of which can form highly toxic reactive intermediates (Overby et al., 1992). Dehydrogenases are commonly existed in various human organs and tissues. Among them, the trimethylamine dehydrogenase of intestinal microorganisms can biologically convert TMA into dimethylamine (DMA) and formaldehyde (Kim et al., 2001; Shi et al., 2005). Nevertheless, whether this metabolic pathway can be realized in human respiratory tract has not been studied yet.

Harmful exogenous pollutants in human body may be detoxified by CYP-catalyzed or non-CYP-mediated biotransformation, or may be activated to become more toxic substances. Pollutant toxicity in respiratory tract frequently results from in situ metabolic activation, and the toxicity of exogenous pollutant tightly links with its metabolic fate in the target organ (Ding and Kaminsky, 2003; Strolin Benedetti et al., 2006). However, during the process of exposure to exogenous pollutant and metabolic activation, organism damage and oxidative stress may also be triggered, which results in adverse effects on corresponding organ or leads to diseases. In vitro metabolism of BEAS-2B cells showed that 5-hydroxymethylfurfural (5-HMF) in cigarette smoke extract could be quickly eliminated under the mediation of CYP2A13 to form 5-HMF acid, which was more toxic than 5-HMF in BEAS-2B cells (Ji et al., 2018). Nilutamide, which can induce pulmonary interstitial fibrosis, was involved in reductive metabolism and redox-cycling, leading to uncontrolled generation of reactive oxygen species (ROSs) (Berger et al., 1992). Polycyclic aromatic hydrocarbons and 2,3,7,8-tetrachlorodibenzo-p-dioxin can cause the up-regulation of CYP1A enzymes in respiratory tract cells, which promoted the release of ROSs and the induction of oxidative stress, leading to inflammation and pulmonary diseases (Aboutabl et al., 2009; Labitzke et al., 2007). However, few studies were carried out on the oxidative stress of respiratory tract induced by volatile organic amines, especially on the metabolic toxicity of TMA in respiratory tract.

Besides being an air pollutant, TMA is also an important metabolite of human physiological activity. Researches have revealed that human gut microbes were implicated in metabolizing choline to TMA, which was subsequently oxidized to trimethylamine-N-oxide by hepatic flavin-containing monooxygenase 3 before excretion via urine (Wang et al., 2011). The metabolite trimethylamine-N-oxide is widely believed to be associated with increased risk of atherosclerosis (Velasquez et al., 2016; Wang et al., 2015). Additionally, abnormal levels of TMA in blood, urine and sweat have been proven to be associated with numerous human disease pathologies, including kidney damage, hepatocellular carcinoma, cardiovascular diseases, and neuropsychiatric disorders (Pelliceiari et al., 2011; Tang et al., 2015). Therefore, whether the metabolism and toxic effects of exogenous TMA entering the human body through the respiratory tract are like that of endogenous TMA remains to be further investigated.

In this study, to explore the toxicity related to the metabolic fate of TMA in respiratory tract, cytotoxicity and ROS generation were examined following exposure of bronchial epithelial cells (16HBE) to TMA. Volatile intermediates of TMA in the headspace of cells were qualitatively and quantitatively analyzed using a Proton Transfer Reaction-Time of Flight-Mass Spectrometer (PTR-TOF-MS) and Proton Transfer Reaction-Quadrupole-Mass Spectrometer (PTR-QMS) in real time. Furthermore, the major metabolites of TMA in cells and culture media solution were also identified, by coupling the non-targeted detection of direct injection with targeted detection of amine-containing metabolites labeled with dansyl chloride using Ultra High Performance Liquid Chromatography coupled with Quadrupole-Time-of-Flight Mass Spectrometer (UPLC-QTOF-MS). Finally, the possible metabolic pathway and mechanism of TMA exposed to 16HBE cells were initially revealed. The toxic effects of TMA metabolism on the respiratory tract were comprehensively demonstrated by combining the results of cytotoxicity with oxidative stress. This is a rare study of the toxic effects of organic amines on the human respiratory system from the perspective of toxicity of pollutant metabolites, rather than just the pollutant itself.

2. Materials and methods

2.1. Chemicals and reagents

Trimethylamine (30 wt% in H_2O, AR) was purchased from Aladdin (Shanghai, China). Danysl chloride, benzylamine, tetraethylammonium chloride and sodium carbonate/sodium bicarbonate buffer were purchased from J&K Scientific (Beijing, China). HPLC-grade ammonium formate and formic acid were obtained from CNW (Technologies GmbH). HPLC-grade methanol (MeOH) and acetonitrile (ACN) were purchased from Merck (Darmstadt, Germany). Water was purified using a Milli-Q system (Research Water Purification Technology, Xiamen, China). The specifications and purity of these chemicals are detailed in Table S1 in Supporting Information (SI).

2.2. Cell culture and cell viability assay

Human bronchial epithelial cell line (16HBE) was obtained from the Chinese Academy of Cell Resource Center (Shanghai, China). Cell culture procedure is provided in SI.

Cell viability was assayed to investigate the cytotoxicity of TMA on respiratory tract cells and determine the exposure concentrations of TMA for the subsequent metabolic studies. A series of TMA concentrations (10.15, 20.30, 30.45, 40.60, 50.75, 60.90, 71.05, 81.20, 91.35 mM) were chosen as exposure groups, and fresh media without the addition of TMA were used as control groups. The detailed procedure is also provided in SI.

2.3. Detection of ROSs

The ROSs were evaluated by staining 16HBE cells in 96-well plates with an oxidation-sensitive fluorescent probe DCFH-DA according to the manufacturer's protocol. 16HBE cells were exposed to TMA (10.15, 20.30, 40.60, 60.90 and 91.35 mM) for 24 h, and the cells treated without TMA were set as the control groups. The detailed test procedure is provided in SI.

2.4. Qualitative and quantitative detection of volatile metabolites of TMA

The cells were exposed to 10.15 mM TMA and cultured in 25 cm^2 cell culture flasks, and the cells without TMA addition were set as the control. The volatile metabolites of TMA in the headspace of cell culture flasks were qualitatively and quantitatively analyzed using PTR-TOF-MS 1000 (Ionicon Analytik GmbH, Innsbruck, Austria) and PTR-QMS 300 (Ionicon Analytik GmbH, Innsbruck, Austria), respectively. The detailed detection procedure is provided in SI.

2.5. Detection of TMA metabolites in cells and culture media

2.5.1. Extraction and pretreatment

The metabolites of TMA in cells and culture media were also analyzed by choosing TMA concentrations of 10.15 and 32.45 mM based on the results of cell viability assay, which corresponded to low and high concentration exposures of TMA in 16HBE cells. The cells were exposed to TMA for 2 and 24 h, while the cells without TMA were set as the control group. After exposure of TMA, the samples were collected, extracted, and pretreated as provided procedure showed in SI.

2.5.2. UPLC-QTOF-MS analysis

TMA metabolites in the cells and culture media were determined using Agilent 1290 Infinity II Ultra High-Performance Liquid Chromatography system coupled with 6545 Quadrupole Time-of-Flight Mass Spectrometer (UPLC-QTOF-MS, Agilent, USA). The liquid chromatography system was equipped with a G7120 binary pump, a G7167B vial sampler, and a G7116B column comp. The drying gas temperature was maintained at 350 °C with a flow rate of 8 L min^{-1}. The nebulizer was set at 35 psig, and the sheath gas temperature was held at 375 °C with a flow rate of 12 L min^{-1}. The nozzle voltage was set at 1500 V for Dual AJS ESI source, and the capillary voltage was set at 3500 V. The fragmentor voltage was set at 150 V, and the skimmer was 65 V. The instrument was set to acquire over a mass-to-charge ratio (m/z) range from 30 to 1100 with the MS acquisition rate of 2 Hz. The samples used for analysis of TMA metabolites were divided into two parts, one portion was used for direct injection analysis, and another was used for indirect identification after derivatization with dansyl chloride. The detailed procedures are provided in SI.

3. Results and discussion

3.1. Effects of TMA on cell viability and ROS generation

To characterize the cytotoxic effect of TMA on respiratory tract and determine the suitable TMA exposure concentration for the subsequent metabolic studies, the viability of 16HBE cells exposed to various concentrations of TMA was measured using cell counting kit-8 (CCK-8). As shown in Fig. 1a, TMA exposure decreased the viability of 16HBE cells in a concentration-dependent manner, inducing a significant decrease in cell viability at the concentration of 40.60 mM and above. At lower concentrations of TMA, the cell viability decreased from 94.66% ± 3.11% with 10.15 mM, to 82.29% ± 11.50% with 30.45 mM. The cell viability reached 32.53% ± 8.05% and 6.86% ± 2.49% when the doses of TMA increased to 40.60 and 60.90 mM, respectively. When the concentration of TMA was higher than 60.90 mM, the cell viability tended to level off, indicating that the cells were almost completely lethal (Cai et al., 2019). Based on the fitted curve using Origin Analysis Software, the LC_{50} (Lethal Concentration 50%) of cell viability on TMA exposure was further determined and its concentration was obtained as 36.12 mM, which was higher than the measured LC_{50} of 24.55 mM for methylamine (MA) (Li et al., 2019), suggesting that TMA was less toxic than MA in 16HBE cells. Moreover, the morphological changes induced by the increased TMA in cells included cell membrane damage, cytoplasm vacuolization, changes in cell shape and the increase of floating cell debris (Fig. S1), which was consistent with the results of cell viability (Fig. 1a). Based on these results, to investigate the cellular metabolism of TMA under low and high concentration exposures, the TMA concentration of 10.15 and 32.45 mM were selected for the subsequent experiments, which corresponded to 5% (LC_5) and 40% (LC_{40}) decrease in cell viability.

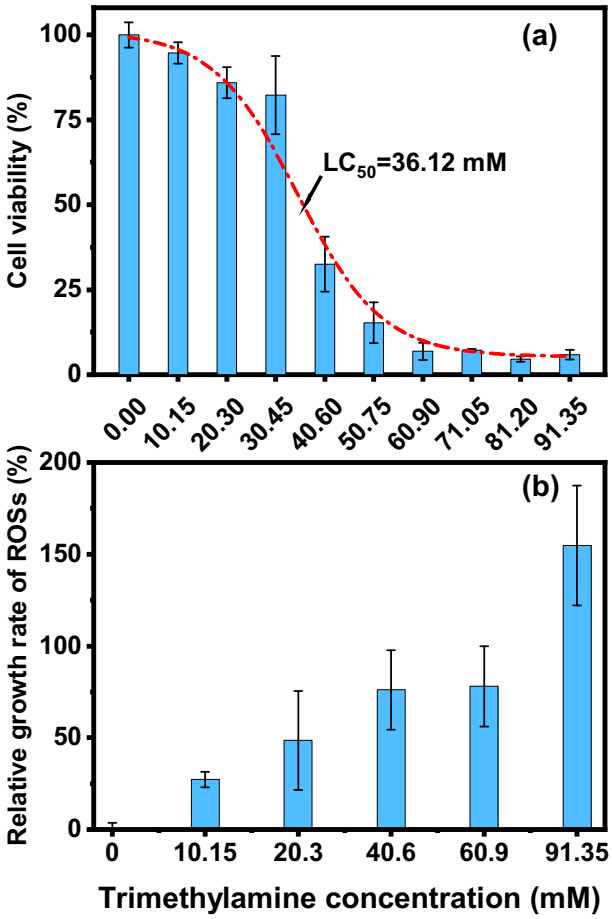

Fig. 1. (a) Cell viability induced by TMA treatment in 16HBE cells for 24 h. The data of cell viability ($n = 3$ wells per treatment group) were fitted to a nonlinear regression curve to determine the LC_{50}; (b) Relative growth rate of intracellular ROSs after exposure to TMA for 24 h. Error bars for each point represent the standard deviation of three replicates.

ROS in cells is a vital marker of oxidative stress after cells were stimulated (Delgado-Roche and Mesta, 2020; Larosa and Remacle, 2018). Therefore, the level of ROSs in cells characterizes the degree of cellular oxidative stress to a certain extent. The more intracellular ROSs increased, the higher degree of cellular oxidative stress occurred (Pizzino et al., 2017; Sies et al., 2017). In this study, as shown in

Fig. 1b, the relative growth rate of ROSs in cells increased with the rising TMA exposure concentration. Within the concentration range of 10.15–60.90 mM, the relative growth rate of ROSs gradually increased from 27.25% ± 4.17% to 78.01% ± 21.88%, which was consistent with the result of cell proliferation toxicity. When the TMA concentration reached 91.35 mM, the intracellular ROSs increased rapidly to 154.82% ± 32.67%, indicating that the cell damage and the cellular oxidative stress was highly serious. Therefore, with the increase of TMA exposure concentration, the relative growth rate of intracellular ROSs increased in a dose-dependent manner, resulting in the severe oxidative damage in 16HBE cells. Generally, decreased cell activity and increased oxidative stress are directly related to exogenous parent compounds. However, the metabolic transformation of exogenous pollutants in cells and their metabolites may also contribute to the above cytotoxic effects.

3.2. Identification and quantification of metabolites of TMA

The variation of the composition and content of volatile intermediates in the cell headspace is a way to directly reflect the changes of cell metabolism (Furuhashi et al., 2020; Liu et al., 2019). In this study, to understand the metabolic changes of TMA during the cell exposure process, PTR-TOF-MS and PTR-QMS were both used to identify and measure the level of volatile intermediates in the headspace of cells exposed to the low concentration of TMA (10.15 mM). Based on the full scan results of PTR-QMS data, significant changes in the concentrations of the three volatile compounds with *m/z* of 46, 60, and 74 were observed between the control and exposure groups. According to the qualitative results of PTR-TOF-MS, the precise m/z of these volatile compounds were 46.0651, 60.0808, and 74.0600, which were identified as (C_2H_7N) H+, (C_3H_9N) H+, and (C_3H_7NO) H+, respectively, and the corresponding compounds were identified as dimethylamine (DMA), TMA and *N,N*-dimethylformamide (DMF).

Fig. 2 shows the changes in the concentration of DMA, TMA and DMF in the headspace of cells using PTR-QMS. All obtained results have been deducted background values of headspace samples containing culture medium only. As the cells were exposed to the liquid exogenous compound, the concentration of TMA in the headspace showed a time-dependent decrease in general, from the concentration of 1343.14 ppb at 2 h exposure to 461.76 ppb at 24 h exposure. The gaseous TMA in the headspace was partially released from the TMA solution. According to the Henry's law (Sander, 2015), the gaseous TMA and the dissolved TMA in the medium maintained an equilibrium state. The concentration of TMA in the headspace decreased with the exposure time, meaning that the concentration of TMA in the medium also decreased. This result further indicated that TMA might undergo a certain extent of metabolism in cells during the exposure process. When the exposure time reached 48 h, the gaseous TMA concentration in the headspace gradually increased back to 619.94 ppb. This might reveal that the metabolism of TMA appeared to be a relatively stable state around the exposure time of 24 h.

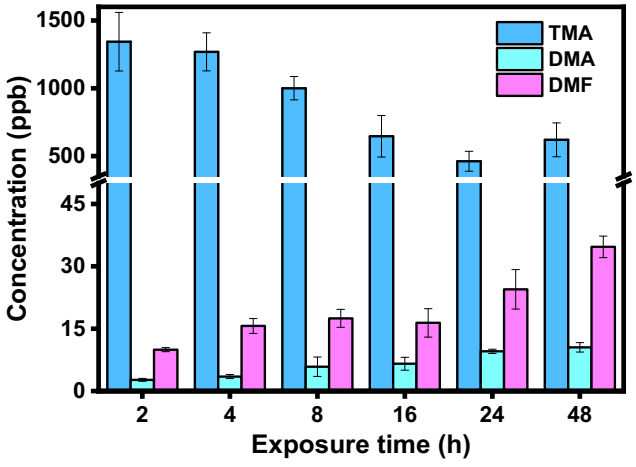

Fig. 2. Concentration variations of TMA and its metabolites DMA, DMF in the headspace of cells with the increase of exposure time using PTR-QMS. Error bars for each point represent the standard deviation of three replicates.

Different from the change trend of TMA, the concentrations of DMA and DMF, the two volatile intermediates detected in the cell headspace, showed a gradual upward trend with the progress of exposure time. DMA increased from 2.70 ppb at 2 h exposure to 10.52 ppb at 48 h exposure, with the concentration increased by 2.89 times. The concentrations of DMF reached 9.96 and 34.68 ppb when the exposure time of TMA reached 2 and 48 h, respectively, increasing by 3.48 times. DMA and DMF, whose concentrations continuously increased during exposure process, were found to be the metabolic intermediates of TMA after metabolic transformation by cells. It was also reasonable to deduce the formation of the two compounds from TMA in the theory of molecular structures. TMA, the compound used to expose to cells, is a tertiary amine with three methyl groups attached to one N-atom. DMA is a secondary amine with two methyl groups attached to one N-atom, which can be obtained by removing a methyl group from TMA. DMF is an amide with two methyl groups and one formaldehyde group attached to one N-atom, which can be obtained by the N-formylation of DMA. According to the previous reports, trimethylamine dehydrogenase existing in intestinal microorganism and marine bacteria can convert TMA into DMA and formaldehyde (Shi et al., 2005; Sun et al., 2019). However, there were few reports about the conversion of TMA to DMF in organisms, and N-formylation of the generated DMA could be the way to form DMF in cells. It was reported that N-formylation of m-Aminobenzoic acid was performed in cell suspension cultures of *Solanum laciniatum* (Syahrania et al., 2000), which showed that N-formylation can occur in the biotransformation of cells. In addition, hydroxylation is an important metabolism that easily occurs after xenobiotics enter the organism (Patten et al., 1997; Su et al., 2015), so DMF may also be generated by further oxidative metabolism by monohydroxylated TMA. Therefore, DMA and DMF were supposed to be the metabolites of TMA, which released into the headspace after the metabolism of respiratory tract cells. It is because that the saturated vapor pressures of DMA and DMF at 25 °C are 2.03×10^5 and 5.16×10^2 Pa, respectively (ACD/Labs, 2016; ECOSAR, 2014), which makes them easy to volatilize into the atmosphere and induce toxic effects on the human body through respiratory exposure (Azuma et al., 2016; Wang et al., 2016).

In addition, it was interesting that the concentration of generated DMF was higher than that of DMA. This can be explained by two main reasons. The first was that TMA might be converted to amide with a higher rate of metabolic conversion. It was reported that TMA had a higher possibility of generating amides in the metabolism of microorganisms, and could even be converted into amino acids (Pattabiraman and Bode, 2011; Siswanto et al., 2016). The second reason was that DMF might be easier to be released into the headspace of the cells than DMA because the Log octanol – water partition coefficient (Log K_{ow}) values of DMA and DMF were − 0.38 and − 1.01, respectively (ACD/Labs, 2016), which could partly explain the difference in the observed 16HBE bioaccumulation. Compared to DMF, DMA was more likely to be accumulated in cells surrounded by the lipid environment. Therefore, DMF could be more easily secreted into the culture medium and then released into the cell headspace.

3.3. Identification of intracellular exogenous metabolites

3.3.1. Non-targeted detection of metabolites without derivatization

Determination of potential TMA metabolites without derivatization in cells and medium samples exposed to TMA for 2 and 24 h was also conducted using an UPLC-QTOF-MS in the full scan mode. No interesting finding was obtained for metabolite analysis in the negative ion mode, but it seemed that some different peaks were found between the

control group and the exposed groups in the positive mode, as shown in Fig. 3a and 3b. However, the specific ions extracted from these different peaks of exposed groups were also found in the control group, and their concentrations were not much different. This was due to the peak drift of some ions in the samples from the control group during separation and analysis by UPLC-QTOF-MS. By means of careful analysis and ion screening to compare the data of the control group and the exposed groups, the specific ion of *m/z* 151.1441 was only detected in the TMA exposure groups at the two exposure time points. That is, two ions appeared at 22.445 and 22.496 min in 2 and 24 h exposure were found in the culture media of both concentration exposure groups, but almost absent in the control group. As shown in Fig. 3c, the intensity of the ion of m/z 151.1441 was only 7.23×10^5 in the sample of the low concentration exposure group of 2 h, while it reached 1.54×10^7 in the high concentration exposure group. The difference in the intensity of this ion between both concentration exposure groups for 24 h (Fig. 3d) was consistent with that for 2 h, indicating that the ion concentration remained stable in the exposed medium samples. Based on the above results, it was speculated that the substance represented by the ion could be a metabolite produced by the transformation of TMA through cell metabolism, for which the further qualitative analysis was required.

The mass spectrum of the extracted ion was further analyzed using Agilent MassHunter software. As shown in Fig. S2, the molecular formula of the ion of m/z 151.1441 was deduced as $C_6H_{18}N_2O_2$, with the matching degree of 99.97%. By using MS/MS mode of UPLC-ESI(+)-QTOF-MS, the ion of m/z 151.1441 generated daughter ion of m/z 76.0756, with a molecular formula of C_3N_9NO. Based on the deduction of the fragmentation mode of the parent ion and the generation mode of the product ion, it was concluded that the parent ion should be *N*,*N*′-Bis(2-hydroxyethyl)-1,2-ethanediaminium, and the daughter ion should be N-Methylethanolamine. Siswanto et al. (2016) mentioned in the proposed mechanism of TMA degradation and mineralization by *Euphorbia milii* that N-Methylethanolamine could be one of the metabolites of TMA. Therefore, the *N*,*N*′-Bis(2-hydroxyethyl)-1,2-ethanediaminium detected in this study, as a kind of hydroxylamines, was similar to the intermediate found in the previous study.

The production of this metabolite may be related to cytochrome P450 (CYP) enzymes in the cells. CYP enzymes mainly distribute in the endoplasmic reticulum and mitochondrial inner membrane of cells (Korobkova, 2015). They are involved in many enzymatic reactions critical to important life processes and also play an important role in the metabolism of xenobiotics and drugs (Hukkanen et al., 2002; Pavek and Dvorak, 2008). They are responsible for the oxidation, reduction, hydrolysis of the exogenous compound in the organism, and transform these exogenous substances from the hydrophobic type to the hydrophilic type which is more easily excreted outside the organism (Bhattacharyya et al., 2014). Heterologously expressed CYP2A13 was active toward many nitrogen compounds, such as hexamethylphosphoramide, N-nitrosodiethylamine, *N*,*N*-dimethylaniline, and *N*-nitrosomethylphenylamine (Su et al., 2000). In this study, under the action of the CYP enzymes in cells, TMA might undergo a certain hydroxylation reaction, temporarily generating hydroxylated TMA. Soon, the resultant intermediates were subjected to the complex reaction of other enzymes, thus finally forming *N*,*N*′-Bis(2-hydroxyethyl)-1,2-ethanediaminium, which was an amine compound containing hydroxyl. The concentration of this compound remained stable in the medium samples exposed for 2 and 24 h, indicating that 16HBE cells can partially convert TMA to this metabolite in a relatively short time.

3.3.2. Targeted detection of amine-containing metabolites labeled with dansyl chloride

In the human body, endogenous TMA can be metabolized to produce amines with small molecules under the action of multiple dehydrogenases (Chistoserdova, 2011; Yang et al., 1995). Herein, dansylation labeling was used to determine the underlying amine-containing metabolites in the media and cells exposed to TMA (Chen et al., 2019; Guo and Li, 2009). Interestingly, two ions, *m/z* 265.1012 and m/z 279.1169, were detected in TMA-exposed 16HBE cells and culture

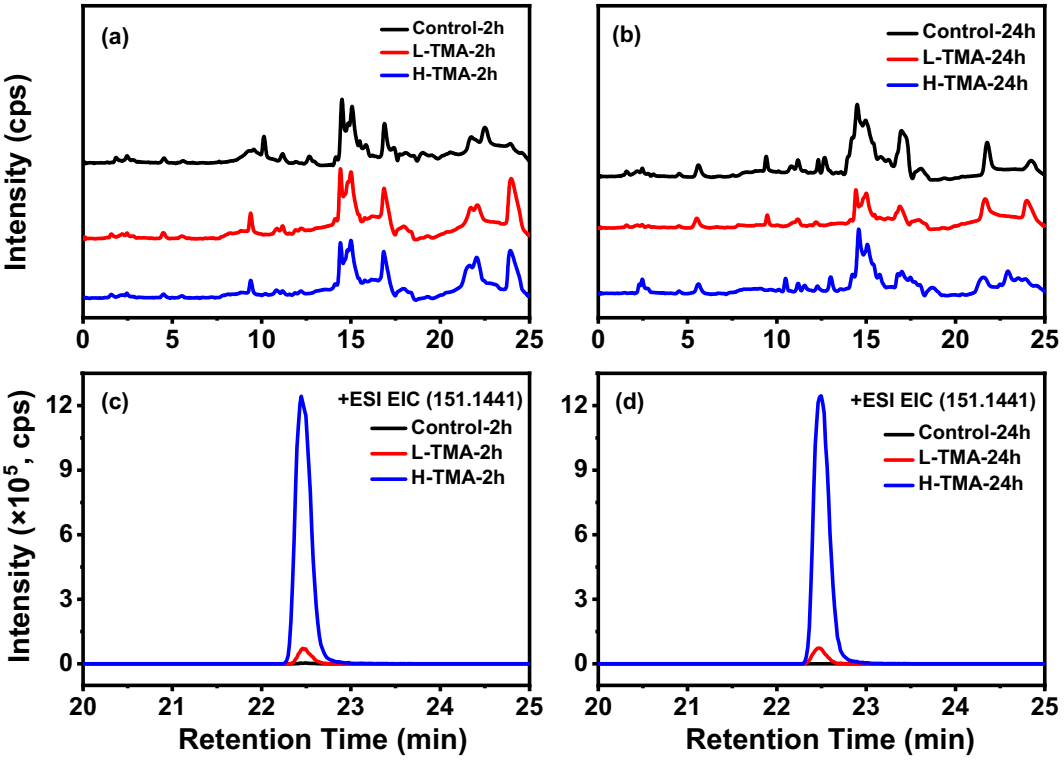

Fig. 3. Total ion chromatograms of extracted organics from the culture media exposed to low concentration and high concentration TMA (L-TMA and H-TMA) and control group for 2 h (a) and 24 h (b) using UPLC-QTOF-MS operated in the full scan mode. Extraction ion chromatograms (*m/z* 151.1441) of extracted organics from the culture media exposed to low concentration and high concentration TMA (L-TMA and H-TMA) and control group for 2 h (c) and 24 h (d).

media by LC-ESI(+)-QTOF-MS, and the ion abundances are obviously different between the control and the exposed groups (Fig. S3). The m/z 265.1012 was presumed to be dansylated-methylamine (DNS-MA) with a formula of $C_{13}H_{16}N_2O_2S$ and with theoretical [M + H] + of m/z 265.1005. The m/z 279.1172 was presumed to be dansylated-dimethylamine (DNS-DMA) with a formula of $C_{14}H_{18}N_2O_2S$ and with theoretical [M + H] + of m/z 279.1162. The identification of these intermediates was confirmed by comparison with standard substances. Therefore, the detected peak of m/z 265.1012 was confirmed as DNS-MA and the peak of m/z 279.1169 was DNS-DMA, which were the derivatives of TMA metabolites.

Figs. 4 and S4 also show the extraction ion spectrum of DNS-MA (m/z 265.1012) and DNS-DMA (m/z 279.1169) in cells and culture media samples for 2 and 24 h of TMA exposure. Through the integration of the above extracted ion spectrum and the calculation of the peak area, the relative quantification of the MA and DMA in the cells and media exposed to TMA was performed. As Fig. S5 shows, the response of MA detected in the cells exposed to high concentration of TMA was distinctly higher than that of the control group and low concentration exposure group, indicating that the production of metabolite MA increased gradually with the increased concentration of TMA exposure at 2 and 24 h. However, the MA response in culture medium of high concentration exposure group was obviously lower than that in control group and low concentration exposure group, which was inconsistent with the results of MA in the cell samples. Generally, exogenous compounds need to go through the processes of contact and absorption by cells before they were metabolized by organisms (Aouida et al., 2003; Muelas et al., 2020). Thus, for cells cultured in vitro, TMA in solution also had a process of transferring from culture medium to cells. Therefore, there were often more metabolites with higher concentration produced in cells, and only a small number of metabolites would be secreted or leaked out of the cells, since the metabolic process of TMA occurred in cells. As such, this can fully explain that MA presented low level in the medium, but high concentration in the cells as exposed to high concentration of TMA.

In addition, it can be found that the response trends of DMA (Fig. S5b) in the samples were similar to MA (Fig. S5a), indicating that they showed the synergistic changes during the metabolism of TMA. Although certain concentrations of MA and DMA were also present in the control group, they were small molecules that might be produced during normal cellular metabolism process. However, the MA and DMA in the cell samples of the exposed group were obviously higher than those in the control group, despite the former without MA and DMA added. Therefore, this also further illustrated that the addition of TMA and the metabolic transformation of TMA by cells caused the increased MA and DMA in the cell samples. With the increase of exposure time, the levels of MA and DMA rose in cells, revealing that the generated concentration of TMA metabolites had a time-dependent effect.

To reflect the actual changes of TMA metabolites, the corrected response changes of MA and DMA after subtracting the response intensity of the control group were also illustrated (Fig. 5). Within 24 h of exposure to low concentration of TMA, MA and DMA gradually accumulated in the cells. However, MA and DMA showed different trends under high concentration exposure. MA increased slowly with the increase of exposure time, while DMA showed a decreasing trend with the increase of exposure time. In addition, comparing the intensity response of MA and DMA, we can find that the content of DMA was at least 5 times higher than that of MA. Although both DMA and MA were the amine metabolites of TMA in cells, the content of the former was higher than that of the latter. This result indicated that TMA may be converted to DMA preferentially during the metabolic process, and MA could be a further metabolite. The decreased DMA under the high concentration exposure meant that DMA may undergo some further metabolism. Therefore, MA should be the metabolite of DMA, which explained the increase in MA content and the decrease in DMA content.

Summarizing the above analysis, we believed that TMA exposure had toxic effects on cells, and the cells also had some detoxification and metabolism effects on TMA. When the dansylation labeling method was used to detect amines in cell samples, we found that the levels of MA and DMA showed surprising responses in the exposed cells. It was

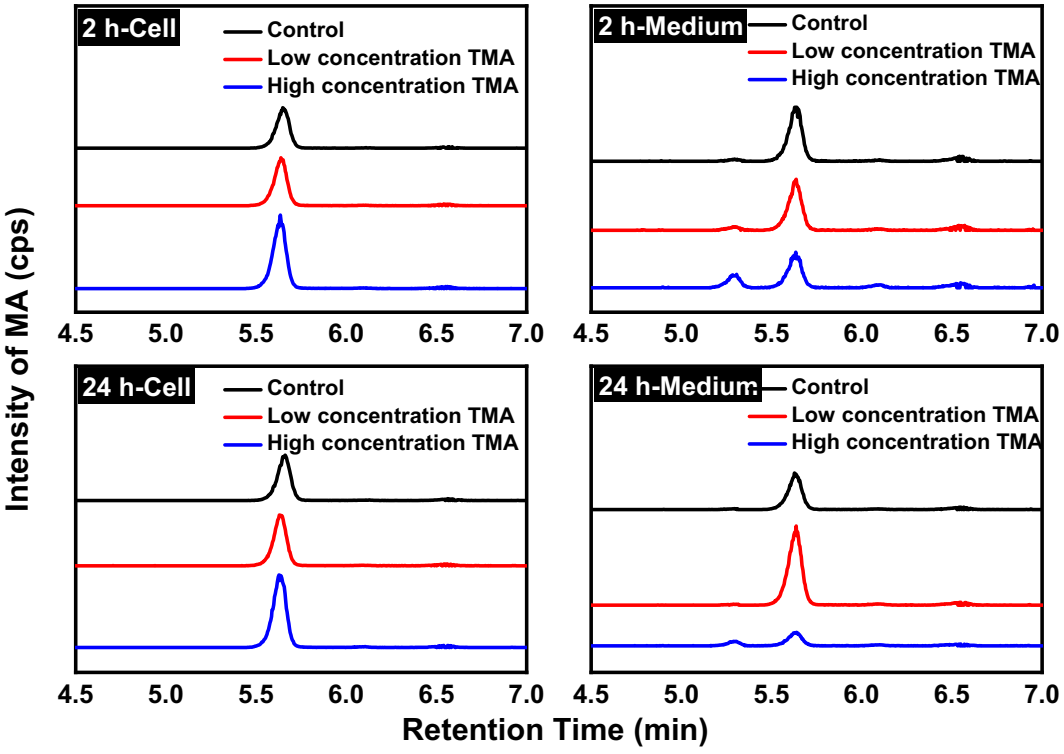

Fig. 4. Extraction ion spectrum of MA labeled with DNS in cells and culture media exposed to low concentration and high concentration TMA and control group for 2 and 24 h.

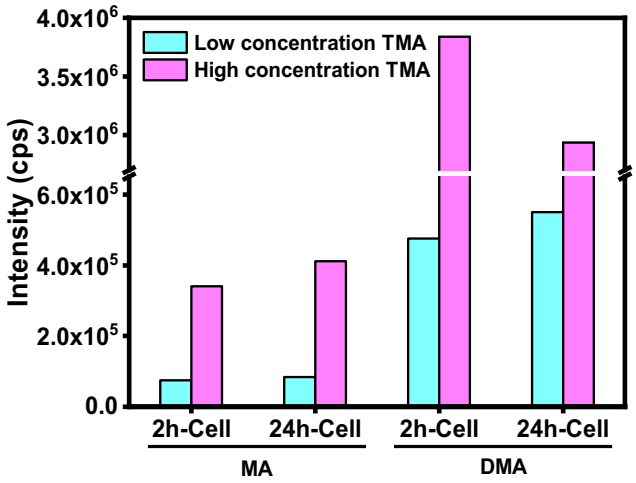

Fig. 5. Corrected response intensity of MA and DMA labeled with DNS from cell samples exposed to low concentration and high concentration TMA for 2 and 24 h (The results were subtracted the response intensity of the control group).

because that under the effect of cell metabolism, TMA was first metabolized to DMA, and then DMA was further metabolized to MA. This metabolic process always followed the principle of demethylation, indicating that demethylase or TMA dehydrogenase was existed in 16HBE cells, which promoted the demethylation metabolism of TMA. This metabolic pathway of TMA also appeared in the metabolic system of some microorganisms. For instance, in some methylotrophs lived in marine environments, TMA dehydrogenase catalyzed the dehydrogenation of TMA directly to form DMA and formaldehyde (Sun et al., 2019), afterwards DMA was further demethylated to MA and then ammonia by a series of dehydrogenase enzymes.

3.4. Proposed metabolic pathway and increased toxicity of TMA in 16HBE cells

Based on the identified metabolites of TMA in the cell headspace and the cell culture solution, the metabolic mechanism of TMA in 16HBE cells was proposed as shown in Fig. 6. During the exposure process of TMA to cells, TMA was in contact with the cell surface in culture medium and partly absorbed by cells. Inside the cells, TMA was metabolized by dehydrogenase to produce DMA, which was then metabolized into MA. In the cell headspace, significant concentration changes of DMA in the exposed group were also detected, indicating that DMA was a key metabolite with certain volatilization. According to predecessors' researches, MA can be further metabolized to produce ammonia and formaldehyde, and finally be mineralized to CO_2 and H_2O (Colby and Zatman, 1973; Kim et al., 2001). However, in this study, by PTR-QMS detection, ammonia and formaldehyde did not show a significant increase in concentration, which may be due to low concentration or more polar property of the secondary metabolite MA. DMF was also found to be a metabolite of another metabolic route of TMA, which was identified in the cell headspace. It was an important intermediate of TMA that was easily secreted into the atmosphere, because its metabolic reaction substrate can be TMA or DMA. On the one hand, the generated DMA can directly form DMF by N-formylation. On the other hand, TMA may first generate intermediate monohydroxylated TMA by oxidation reaction, and then be further oxidized to generate monoaldehyde-based TMA, which is just DMF. *N*,*N*′-Bis(2-hydroxyethyl)-1,2-ethanediaminium was detected in cells and culture media exposed to TMA, indicating that it may be another important metabolite in TMA metabolism. Because it contains two N-groups, it was considered that the precursor metabolite of *N*,*N*′-Bis(2-hydroxyethyl)-1,2-ethanediaminium is N-Methylethanolamine, which was confirmed in early report that N-Methylethanolamine may be one of the main metabolites of TMA (Siswanto et al., 2016). Therefore, the production of N-Methylethanolamine may be achieved by the demethylation and hydroxylation of TMA.

For the formation of DMF and *N*,*N*′-Bis(2-hydroxyethyl)-1,2-ethanediaminium, it was believed that CYP enzymes may be involved in the metabolism. CYP enzymes are important metabolic enzymes in the human body, which preferentially catalyze oxidations on hard nucleophilic centers, such as carbon atoms (Oesch et al., 2019). CYP enzymes can convert exogenous pollutants into more hydrophilic metabolites with hydroxyl or aldehyde groups by oxidation, and these metabolites are often more toxic since they are easier to be absorbed and utilized by cells (Oesch-Bartlomowicz and Oesch, 2007). Previous studies have shown that when mice inhaled TMA for 2 h, the LC_{50} of DMF was obtained as 2880 ppm, which was much lower than the LC_{50}

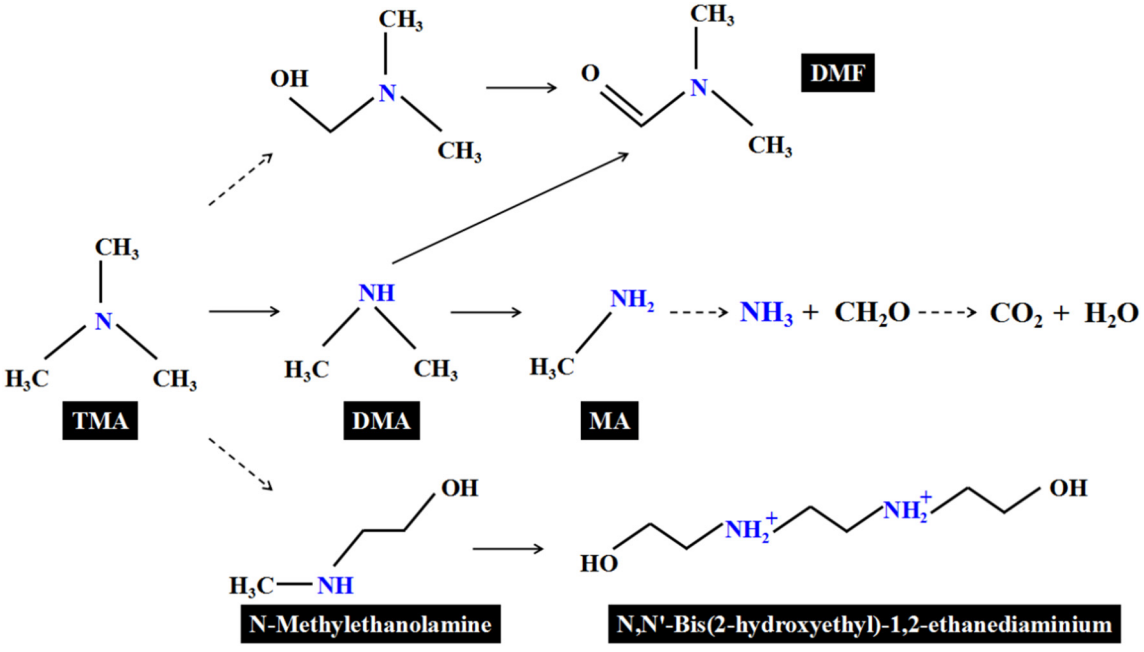

Fig. 6. The proposed metabolic pathways of TMA in 16HBE cells.

of TMA (7790 ppm) (Rotenberg and Mashbits, 1967), indicating that the inhalation toxicity of DMF was higher than that of TMA. In addition, DMF exposure can result in mitochondrial dysfunction and glutathione depletion, which were closely related to the generation of ROSs (Xu et al., 2020). Moreover, as a stable organic pollutant in the environment withstanding various physical and chemical conditions (Xiao et al., 2016), DMF was classified as group 2A carcinogen by International Agency for Research on Cancer (IARC) in 2016 (IARC, 2016). Hence, more attention should be paid to DMF produced by the biotransformation of TMA, since it may cause more serious cytotoxicity in the respiratory tract. *N*,*N*′-Bis(2-hydroxyethyl)-1,2-ethanediaminium is a kind of hydroxylamines containing two hydroxyl groups, and there are few toxicity studies and toxicological data about it. Although there is no direct evidence that *N*,*N*′-Bis(2-hydroxyethyl)-1,2-ethanediaminium is more toxic than TMA, diethanolamine and 2-dimethylaminoethanol, both of which belong to hydroxylamines, have been found to be toxic and irritating to the environment and organisms (Blum et al., 1972; Cronheim and Toekes, 1959). Thus, the metabolite *N*,*N*′-bis(2-hydroxyethyl)-1,2-ethylenediamine may also affect the toxic effects of respiratory tract cells.

The deep oxidation of TMA demethylation was the main metabolic pathway, in which DMA and MA were important intermediates, and they were often considered to have lower toxicity than the parent TMA previously. However, the results of animal experiments showed that the LC_{50} of DMA and MA for 2 h inhalation exposure to mice were obtained of 7560 and 1890 ppm, respectively (Mezentseva, 1956), revealing that the toxicity of demethylated metabolites was higher than that of TMA. This can be reasonably explained in some respects. Compared with TMA, DMA and MA contain fewer methyl groups and have lower Log K_{ow}, thus they were so more hydrophilic that they can be absorbed and utilized by cells, inducing greater toxic effects on cells. Besides, the measured LC_{50} of TMA (36.12 mM) for 24 h exposure was higher than that of MA (24.55 mM), which further showed that MA was more toxic than TMA, stimulating the overproduction of ROSs in cytoplasm and mitochondria of 16HBE cells (Li et al., 2019). Studies have shown that TMA can lead to adverse respiratory reactions such as degeneration of tracheal mucosa, bronchial inflammation and decreased respiratory rate in rats and mice (USEPA, 2009), and even lead to reproductive toxicity by inhibiting the synthesis of macromolecules in mouse embryos (Guest et al., 1994). In addition, elevated TMA in vivo can cause progressive tubulointerstitial fibrosis and dysfunction in humans (Bain et al., 2006), induce endoplasmic reticulum stress associated with metabolic diseases such as obesity or diabetes (Hummasti and Hotamisligil, 2010), and result in depression, seizures, and behavioral disorders (Chang et al., 2013). The metabolism of TMA in the body was active and complex (Chhibber-Goel et al., 2016), which may cause its metabolites to induce the above toxic effects in vivo together with TMA. Herein, our research also found that TMA may be metabolized into more toxic metabolites in bronchial epithelial cells (16HBE), which thus together induce more serious toxic effects on cells and even the respiratory tract with a synergetic effect.

4. Conclusions

It is of great significance to understand the toxic effects of volatile organic amines in the atmosphere on the human respiratory tract and their metabolic transformation mechanisms in vivo. Therefore, taking a typical volatile TMA with a characteristic fishy odor as an example, the changes in cell viability and ROS production during the exposure of TMA in respiratory epithelial cells 16HBE cultured in vitro were studied. Results showed that the cell viability decreased and ROS generation increased in a concentration-dependent manner. Interestingly, while 16HBE cells suffered from the toxic effects of TMA-induced oxidative stress, they also produce certain metabolic effects on TMA. TMA volatilized in the apical air of the cells was depleted in a time-dependent manner by approximately 65% after 24 h of exposure, and DMA was found to be the key metabolite. In addition to obtaining DMA and MA products by demethylation, TMA may also be oxygenated to form DMF or *N*,*N*′-Bis(2-hydroxyethyl)-1,2-ethanediaminium through N-formylation or hydroxylation with the participation of CYP enzymes. These obtained metabolites had higher toxicity than TMA itself, and DMF was also classified as a carcinogen. Therefore, the oxidative stress and necrosis of cells during exposure may be the synergistic effects of TMA and its metabolites, rather than just the effects of TMA itself. Our work provides a valuable insight into the metabolic mechanism of volatile organic amines in human respiratory tract cells and reveals the toxic synergistic effects of metabolites as well as original parent atmospheric organic amines. However, further researches may be needed for verification and improvement, such as experiments on animals or human samples.

CRediT authorship contribution statement

Zhilin Qiu: Methodology, Formal analysis, Writing – original draft. **Guiying Li:** Writing – review & editing, Supervision. **Taicheng An:** Conceptualization, Supervision.

Declaration of competing interest

The authors declare that they have no known competing financial interests or personal relationships that could have appeared to influence the work reported in this paper.

Acknowledgements

This work was supported by National Natural Science Foundation of China (41877363, 42020104001 and U1901210), National Key Research and Development Project (2019YFC1804504 and 2019YFC1804503), Local Innovative and Research Teams Project of Guangdong Pearl River Talents Program (2017BT01Z032).

Appendix A. Supplementary data

Supplementary data to this article can be found online at https://doi.org/10.1016/j.scitotenv.2021.146915.

References

Aboutabl, M.E., Zordoky, B.N.M., El-Kadi, A.O.S., 2009. 3-Methylcholanthrene and benzo(a)pyrene modulate cardiac cytochrome P450 gene expression and arachidonic acid metabolism in male Sprague Dawley rats. Brit. J. Pharmacol. 158, 1808–1819.
ACD/Labs. ACD/Labs Percepta, Inc.,Toronto, Ontario, Canada., 2016.
American, I.H.A., 2005. "Trimethylamine", in The Workplace Environment Exposure Level Guide, 2005 Revision, AIHA, Fairfax, VA.
Aouida, M., Tounekti, O., Belhadj, O., Mir, L.M., 2003. Comparative roles of the cell wall and cell membrane in limiting uptake of xenobiotic molecules by Saccharomyces cerevisiae. Antimicrob. Agents. Ch. 47, 2012–2014.
Azuma, K., Endo, G., Endo, Y., Nara, K., Harada, K., Hori, H., Horie, S., Horiguchi, H., Ichiba, M., Ichihara, G., Ikeda, M., Ishitake, T., Ito, A., Iwasawa, S., Kamijima, M., Karita, K., Kawai, T., Kawamoto, T., Koizumi, A., Kumagai, S., Kusaka, Y., Miyagawa, M., Morimoto, Y., Nagano, K., Nase, T., Nomiyamal, T., Omae, K., Sato, K., Okuda, H., Sakurai, H., Sobue, T., Suwazono, Y., Takebayashi, T., Takeshita, T., Takeuchi, A., Tanaka, M., Tanaka, S., Tsukahara, T., Tsunoda, M., Ueno, S., Yamano, Y., Yamauchi, T., Yano, E., Japan Soc Occupational, H., 2016. Occupational exposure limits of lead, dimethylamine, n-butyl-2,3-epoxypropyl ether, and 2-ethyl-1-hexanol and carcinogenicity and occupational sensitizer classification. J. Occup. Health 58, 385–387.
Bain, M.A., Faull, R., Fornasini, G., Milne, R.W., Evans, A.M., 2006. Accumulation of trimethylamine and trimethylamine-N-oxide in end-stage renal disease patients undergoing haemodialysis. Nephrol. Dial. Transpl. 21, 1300–1304.
Berger, V., Berson, A., Wolf, C., Chachaty, C., Fau, D., Fromenty, B., Pessayre, D., 1992. Generation of free radicals during the reductive metabolism of nilutamide by lung microsomes: possible role in the development of lung lesions in patients treated with this anti-androgen. Biochem. Pharmacol. 43, 654–657.
Bhattacharyya, S., Sinha, K., Sil, P.C., 2014. Cytochrome P450s: mechanisms and biological implications in drug metabolism and its interaction with oxidative stress. Curr. Drug Metab. 15, 719–742.
Blum, K., Huizenga, C.G., Ryback, R.S., Johnson, D.K., Geller, I., 1972. Toxicity of diethanolamine in mice. Toxicol. Appl. Pharm. 22, 175–185.
Cai, L., Qin, X.J., Xu, Z.H., Song, Y.Y., Jiang, H.J., Wu, Y., Ruan, H.J., Chen, J., 2019. Comparison of cytotoxicity evaluation of anticancer drugs between real-time cell analysis and CCK-8 method. ACS Omega 4, 12036–12042.

Chang, W.P., Wu, J.J.S., Shyu, B.C., 2013. Thalamic modulation of cingulate seizure activity via the regulation of gap junctions in mice thalamocingulate slice. PLoS One 8, e62952.
Chen, Y.T., Huang, H.C., Hsieh, Y.J., Fu, S.H., Li, L., Chen, C.L., Chu, L.J., Yu, J.S., 2019. Targeting amine- and phenol-containing metabolites in urine by dansylation isotope labeling and liquid chromatography mass spectrometry for evaluation of bladder cancer biomarkers. J. Food Drug Anal. 27, 460–474.
Chhibber-Goel, J., Gaur, A., Singhal, V., Parakh, N., Bhargava, B., Sharma, A., 2016. The complex metabolism of trimethylamine in humans: endogenous and exogenous sources. Expert Rev. Mol. Med. 18, e8.
Chistoserdova, L., 2011. Modularity of methylotrophy, revisited. Environ. Microbiol. 13, 2603–2622.
Colby, J., Zatman, L.J., 1973. Trimethylamine metabolism in obligate and facultative methylotrophs. Biochem. J. 132, 101–112.
Cronheim, G.E., Toekes, I.M., 1959. The effect of 2-dimethylaminoethanol (deanol) on anaphylactoid edema in rats. J. Pharmacol. Exp. Ther. 127, 167–170.
Dahl, A.R., Bond, J.A., Petridou-Fischer, J., Sabourin, P.J., Whaley, S.J., 1988. Effects of the respiratory tract on inhaled materials. Toxicol. Appl. Pharm. 93, 484–492.
Delgado-Roche, L., Mesta, F., 2020. Oxidative stress as key player in severe acute respiratory syndrome coronavirus (SARS-CoV) infection. Arch. Med. Res. 51, 384–387.
Ding, X.X., Kaminsky, L.S., 2003. Human extrahepatic cytochromes P450: function in xenobiotic metabolism and tissue-selective chemical toxicity in the respiratory and gastrointestinal tracts. Annu. Rev. Pharmacol. Toxicol. 43, 149–173.
ECOSAR, 2014. http://www.epa.gov/oppt/newchems/tools/21ecosar.htm.
Foth, H., 1995. Role of the lung in accumulation and metabolism of xenobiotic compounds–implications for chemically induced toxicity. Crit. Rev. Toxicol. 25, 165–205.
Furuhashi, T., Ishii, R., Onishi, H., Ota, S., 2020. Elucidation of biochemical pathways underlying VOCs production in A549 cells. Front. Mol. Biosci. 7, 116.
Ge, X., Wexler, A.S., Clegg, S.L., 2011. Atmospheric amines–part I. A review. Atmos. Environ. 45, 524–546.
Guest, I., Cyr, D.G., Varma, D.R., 1994. Mechanism of trimethylamine-induced inhibition of macromolecular synthesis by mouse embryos in culture. Food Chem. Toxicol. 32, 365–71.
Guo, K., Li, L., 2009. Differential C-12/C-13-isotope dansylation labeling and fast liquid chromatography/mass spectrometry for absolute and relative quantification of the metabolome. Anal. Chem. 81, 3919–3932.
Hukkanen, J., Pelkonen, A., Hakkola, J., Raunio, H., 2002. Expression and regulation of xenobiotic-metabolizing cytochrome P450 (CYP) enzymes in human lung. Crit. Rev. Toxicol. 32, 391–411.
Hummasti, S., Hotamisligil, G.S., 2010. Endoplasmic reticulum stress and inflammation in obesity and diabetes. Circ. Res. 107, 579–591.
IARC, 2016. Monographs on the evaluation of carcinogenic risks to humans. In: Some Industrial Chemicals 2016. International Agency for Research on Cancer, Lyon, France.
Ji, M., Zhang, Z., Li, N., Xia, R., Wang, C., Yu, Y., Yao, S., Shen, J., Wang, S.L., 2018. Identification of 5-hydroxymethylfurfural in cigarette smoke extract as a new substrate metabolically activated by human cytochrome P450 2A13. Toxicol. Appl. Pharm. 359, 108–117.
Kamarulzaman, N.H., Le-Minh, N., Fisher, R.M., Stuetz, R.M., 2019. Quantification of VOCs and the development of odour wheels for rubber processing. Sci. Total Environ. 657, 154–168.
Kim, S.G., Bae, H.S., Lee, S.T., 2001. A novel denitrifying bacterial isolate that degrades trimethylamine both aerobically and anaerobically via two different pathways. Arch. Microbiol. 176, 271–277.
Kinney, L.A., Burgess, B.A., Chen, H.C., Kennedy, G.L., 1990. Inhalation toxicology of trimethylamine. Inhal. Toxicol. 2, 41–51.
Koehl, W., Amin, S., Staretz, M.E., Ueng, Y.F., Yamazaki, H., Tateishi, T., Guengerich, F.P., Hecht, S.S., 1996. Metabolism of 5-methylchrysene and 6-methylchrysene by human hepatic and pulmonary cytochrome P450 enzymes. Cancer Res. 56, 316–324.
Korobkova, E.A., 2015. Effect of natural polyphenols on cyp metabolism: implications for diseases. Chem. Res. Toxicol. 28, 1359–1390.
Labitzke, E.M., Diani-Moore, S., Rifkind, A.B., 2007. Mitochondrial P450-dependent arachidonic acid metabolism by TCDD-induced hepatic CYP1A5; conversion of EETs to DHETs by mitochondrial soluble epoxide hydrolase. Arch. Biochem. Biophys. 468, 70–81.
Larosa, V., Remacle, C., 2018. Insights into the respiratory chain and oxidative stress. Biosci. Rep. 38, 14.
Li, G., Liao, Y., Hu, J., Lu, L., Zhang, Y., Li, B., An, T., 2019. Activation of NF-kappa B pathways mediating the inflammation and pulmonary diseases associated with atmospheric methylamine exposure. Environ. Pollut. 252, 1216–1224.
Liu, Y., Li, W., Duan, Y., 2019. Effect of H_2O_2 induced oxidative stress (OS) on volatile organic compounds (VOCs) and intracellular metabolism in MCF-7 breast cancer cells. J. Breath Res. 13, 036005.
Mezentseva, N.V., 1956. Materials characterizing the toxicity of dimethylamine. Gig. Sanit. 21, 47–49.
Muelas, M.W., Roberts, I., Mughal, F., O'Hagan, S., Day, P.J., Kell, D.B., 2020. An untargeted metabolomics strategy to measure differences in metabolite uptake and excretion by mammalian cell lines. Metabolomics 16, 107.
Oesch, F., Fabian, E., Landsiedel, R., 2019. Xenobiotica-metabolizing enzymes in the lung of experimental animals, man and in human lung models. Arch. Toxicol. 93, 3419–3489.
Oesch-Bartlomowicz, B., Oesch, F., 2007. 5.08 - Mechanisms of toxification and detoxification which challenge drug candidates and drugs. In: Taylor, J.B., Triggle, D.J. (Eds.), Comprehensive Medicinal Chemistry II. Elsevier, Oxford, pp. 193–214.
Overby, L., Nishio, S.J., Lawton, M.P., Plopper, C.G., Philpot, R.M., 1992. Cellular localization of flavin-containing monooxygenase in rabbit lung. Exp. Lung Res. 18, 131–144.
Pattabiraman, V.R., Bode, J.W., 2011. Rethinking amide bond synthesis. Nature 480, 471–479.
Patten, C.J., Smith, T.J., Friesen, M.J., Tynes, R.E., Yang, C.S., Murphy, S.E., 1997. Evidence for cytochrome P450 2A6 and 3A4 as major catalysts for N'-nitrosonornicotine alpha-hydroxylation by human liver microsomes. Carcinogenesis 18, 1623–1630.
Pavek, P., Dvorak, Z., 2008. Xenobiotic-induced transcriptional regulation of xenobiotic metabolizing enzymes of the cytochrome P450 superfamily in human extrahepatic tissues. Curr. Drug Metab. 9, 129–143.
Pelliceiari, A., Posar, A., Cremonini, M.A., Parmeggiani, A., 2011. Epilepsy and trimethylaminuria: a new case report and literature review. Brain and Development 33, 593–596.
Pitts Jr., J.N., Grosjean, D., Van Cauwenberghe, K., Schmid, J.P., Fitz, D.R., 1978. Photooxidation of aliphatic amines under simulated atmospheric conditions: formation of nitrosamines, nitramines, amides, and photochemical oxidant. Environ. Sci. Technol. 12, 946–953.
Pizzino, G., Irrera, N., Cucinotta, M., Pallio, G., Mannino, F., Arcoraci, V., Squadrito, F., Altavilla, D., Bitto, A., 2017. Oxidative stress: harms and benefits for human health. Oxidative Med. Cell. Longev. 2017, 8416763.
Rotenberg, I.S., Mashbits, F.D., 1967. On the toxic effect of low trimethylamine concentrations. Gigiena truda i professional'nye zabolevaniia 11, 26–30.
Ruangyuttikarn, W., Appleton, M.L., Yost, G.S., 1991. Metabolism of 3-methylindole in human tissues. Drug Metab. Dispos. 19, 977–984.
Sander, R., 2015. Compilation of Henry's law constants (version 4.0) for water as solvent. Atmos. Chem. Phys. 15, 4399–4981.
Seo, S.G., Ma, Z.K., Jeon, J.M., Jung, S.C., Lee, W.B., 2011. Measurements of key offensive odorants in a fishery industrial complex in Korea. Atmos. Environ. 45, 2929–2936.
Serabjit-Singh, C.J., Wolf, C.R., Philpot, R.M., Plopper, C.G., 1980. Cytochrome p-450: localization in rabbit lung. Science 207, 1469–1470.
Shi, W.W., Mersfelder, J., Hille, R., 2005. The interaction of trimethylamine dehydrogenase and electron-transferring flavoprotein. J. Biol. Chem. 280, 20239–20246.
Sies, H., Berndt, C., Jones, D.P., 2017. Oxidative stress, in: Kornberg, R.D. (Ed.), Annual Review of Biochemistry, Vol 86. Annual Reviews, Palo Alto, pp. 715–748.
Silva, P.J., Erupe, M.E., Price, D., Elias, J., Malloy, Q.G.J., Li, Q., Warren, B., Cocker III, D.R., 2008. Trimethylamine as precursor to secondary organic aerosol formation via nitrate radical reaction in the atmosphere. Environ. Sci. Technol. 42, 4689–4696.
Siswanto, D., Chhon, Y., Thiravetyan, P., 2016. Uptake and degradation of trimethylamine by *Euphorbia milii*. Environ. Sci. Pollut. R. 23, 17067–17076.
Stading, R., Chu, C., Couroucli, X., Lingappan, K., Moorthy, B., 2020. Molecular role of cytochrome P4501A enzymes in oxidative stress. Curr. Opin. Toxicol. 20-21, 77–84.
Strolin Benedetti, M., Whomsley, R., Baltes, E., 2006. Involvement of enzymes other than CYPs in the oxidative metabolism of xenobiotics. Expert Opin. Drug Met. 2, 895–921.
Su, G.Y., Letcher, R.J., Crump, D., Gooden, D.M., Stapleton, H.M., 2015. In vitro metabolism of the flame retardant triphenyl phosphate in chicken embryonic hepatocytes and the importance of the hydroxylation pathway. Environ. Sci. Technol. Lett. 2, 100–104.
Su, T., Bao, Z.P., Zhang, Q.Y., Smith, T.J., Hong, J.Y., Ding, X.X., 2000. Human cytochrome p450 CYP2A13: predominant expression in the respiratory tract and its high efficiency metabolic activation of a tobacco-specific carcinogen, 4-(methylnitrosamino)-1-(3-pyridyl)-1-butanone. Cancer Res. 60, 5074–5079.
Sun, J., Mausz, M.A., Chen, Y., Giovannoni, S.J., 2019. Microbial trimethylamine metabolism in marine environments. Environ. Microbiol. 21, 513–520.
Syahrania, A., Panjaitan, T.S., Indrayanto, G., Wilkins, A.L., 2000. N-acetylation and N-formylation of m-aminobenzoic acid by cell suspension cultures of Solanum laciniatum. J. Asian Nat. Prod. Res. 2, 305–309.
Tang, W.H.W., Wang, Z.N., Kennedy, D.J., Wu, Y.P., Buffa, J.A., Agatisa-Boyle, B., Li, X.M.S., Levison, B.S., Hazen, S.L., 2015. Gut microbiota-dependent trimethylamine N-oxide (TMAO) pathway contributes to both development of renal insufficiency and mortality risk in chronic kidney disease. Circ. Res. 116, 448–455.
USEPA, 2009. Acute Exposure Guideline Level (AEGLs) for Trimethylamine (CAS).
Velasquez, M.T., Ramezani, A., Manal, A., Raj, D.S., 2016. Trimethylamine N-oxide: the good, the bad and the unknown. Toxins 8, 11.
Wang, C., Yang, J.H., Lu, D.Z., Fan, Y.S., Zhao, M.R., Li, Z.Y., 2016. Oxidative stress-related DNA damage and homologous recombination repairing induced by N,N-dimethylformamide. J. Appl. Toxicol. 36, 936–945.
Wang, Z., Klipfell, E., Bennett, B.J., Koeth, R., Levison, B.S., Dugar, B., Feldstein, A.E., Britt, E.B., Fu, X., Chung, Y.-M., Wu, Y., Schauer, P., Smith, J.D., Allayee, H., Tang, W.H.W., DiDonato, J.A., Lusis, A.J., Hazen, S.L., 2011. Gut flora metabolism of phosphatidylcholine promotes cardiovascular disease. Nature 472, 57-U82.
Wang, Z., Roberts, A.B., Buffa, J.A., Levison, B.S., Hazen, S.L., 2015. Non-lethal inhibition of gut microbial trimethylamine production for the treatment of atherosclerosis. Cell 163, 1585–1595.
Xiao, J., Chu, S., Tian, G., Thring, R.W., Cui, L., 2016. An eco-tank system containing microbes and different aquatic plant species for the bioremediation of N,N-dimethylformamide polluted river waters. J. Hazard. Mater. 320, 564–570.
Xu, L., Zhao, Q., Luo, J., Ma, W., Jin, Y., Li, C., Hou, Y., Feng, M., Wang, Y., Chen, J., Zhao, J., Zheng, Y., Yu, D., 2020. Integration of proteomics, lipidomics, and metabolomics reveals novel metabolic mechanisms underlying N, N-dimethylformamide induced hepatotoxicity. Ecotox. Environ. Safe. 205, 111166.
Yang, C.C., Packman, L.C., Scrutton, N.S., 1995. The primary structure of Hyphomicrobium X dimethylamine dehydrogenase. Relationship to trimethylamine dehydrogenase and implications for substrate recognition. Eur. J. Biochem. 232, 264–271.
Zhang, W., Ji, Y., Li, G., Shi, Q., An, T., 2019. The heterogeneous reaction of dimethylamine/ammonia with sulfuric acid to promote the growth of atmospheric nanoparticles. Environ. Sci.: Nano 6, 2767–2776.
Zhang, W., Zhong, J., Shi, Q., Gao, L., Ji, Y., Li, G., An, T., Francisco, J.S., 2021. Mechanism for rapid conversion of amines to ammonium salts at the air–particle interface. J. Am. Chem. Soc. 143, 1171–1178.
Zhao, X., Shi, X., Ma, X., Zuo, C., Wang, H., Xu, F., Sun, Y., Zhang, Q., 2020. 2-Methyltetrol sulfate ester-initiated nucleation mechanism enhanced by common nucleation precursors: a theory study. Sci. Total Environ. 723, 137987.